HHS Public Access

Author manuscript

J Viruses. Author manuscript; available in PMC 2016 April 25.

Published in final edited form as:

J Viruses. 2015 ; 2015: . doi:10.1155/2015/646303.

Analogs of LDL Receptor Ligand Motifs in Dengue Envelope and Capsid Proteins as Potential Codes for Cell Entry

Juan Guevara Jr., **Jamie Romo Jr.**, **Troy McWhorter**, and **Natalia Valentinova Guevara***

Biophysics Research Laboratory, Department of Physics and Astronomy, University of Texas at Brownsville, ONE West University Blvd, Brownsville, TX 78520

Abstract

It is established that cell entry of low density lipoprotein particles (LLPs) containing Apo B100 and Apo E is mediated by receptors and GAGs. Receptor ligand motifs, X**BBB**XX**B**X, X**BB**X**B**X, and Ψ**B**ΨX**B**, and mono- and bipartite NLS sequences are abundant in Apo E and Apo B100 as well as in envelope and capsid proteins of Dengue viruses 1–4 (DENV1–4). Synthetic, fluorescence-labeled peptides of sequences in DENV2 envelope protein, and DENV3 capsid that include these motifs were used to conduct a qualitative assessment of cell binding and entry capacity using HeLa cells. DENV2 envelope peptide, Dsp2EP, ^{0564}Gly-Gly^{0595}, was shown to bind and remain at the cell surface. In contrast, DENV3 capsid protein peptide, Dsp3CP, ^{0002}Asn-Gln^{0028}, readily enters HeLa cells and accumulates at discrete loci in the nucleus. FITC-labeled dengue synthetic peptides colocalize with Low Density Lipoprotein-CM-DiI and Apo E-CM-DiI to a degree that suggests that Dengue viruses may utilize cell entry pathways used by LLPs.

Keywords

Apolipoproteins; Cell entry; Dengue virus; Low density lipoprotein; Receptor ligand

INTRODUCTION

The *Flaviviridae* viruses and low-density lipoparticles (LLPs), low-density lipoproteins (LDL), intermediate-density lipoprotein (IDL) and very low-density lipoproteins (VLDL), are unrelated biological entities. Nevertheless, there are many striking similarities between viral particles and LLPs that have been largely overlooked. Flaviviruses and LLPs are similar in a general sense as both include lipids and proteins arranged in roughly spherical structures. Flaviviruses are approximately 500 Å in diameter [1] while LLPs range in size from 250 to 600 Å [2, 3]. Intriguing, proteins of *Flaviviridae* and LLP have similar capacities to enclose, protect, transport, and deliver nucleic acids to cytoplasm and/or cell nucleus [4, 5]. Lipids in both are essential for conformational integrity and functionality of the proteins.

The *Flaviviridae* family includes three genera of positive, single-strand RNA viruses, *Flavivirus*, *Hepacivirus*, and *Pestivirus* [6]. These arthropod-vectored human pathogenic

*Corresponding Author: Natalia Valentinova Guevara, natalia.guevara@utb.edu, Phone: 956-882-6773; Fax: 956-882-6657.

viruses are emerging threats to first world nations [7]. Flaviviruses are characterized by an outer “envelope” that protects and delivers the encapsulated genome. The outer envelope is comprised of a bilayer lipid membrane, derived from the host cell endoplasmic reticulum [8], and two glycoproteins, M and envelope glycoprotein E [9]. In dengue viruses 1–4 (DENV1–4), the outer envelope contains 90 dimers of glycoprotein E each associated with a protein M [1]. Many viruses, including the *Flaviviridae*, use receptor-mediated pathways for cell entry [9]. Clathrin-mediated endocytosis of dengue has been suggested [10–13]. Domain III of the DENV envelope protein is thought to be essential for cell entry; however, specific receptor ligand motifs in dengue structural proteins have not been identified [6–14].

LLPs are characterized by a single molecule of apolipoprotein B100 (Apo B100), multiple copies of apolipoprotein E (Apo E), and other apolipoproteins such as apo C-I, -II, -III, A-I, -II, -IV, and M [15, 16]. LLPs include mainly phospholipids, cholesterol, cholesterol esters, and triglycerides [17, 18], arranged in pseudo-micelles with a monolayer of phospholipid on the surface and a hydrophobic core. Endocytosis, which involves cell surface receptors and clathrin-coated endosomes, was elucidated for LDL and other LLPs first by Brown and Goldstein [19]. Apo B100 and Apo E contain motifs that bind LDL B/E receptors and other proteins of the LDL receptor-related super family (LRPs) [20–23]. Motifs, X**BBB**XX**B**X, X**BB**X**B**X, Ψ**B**ΨX**B**X, and XX**B**XX**B**XXX**BB** (Type I, II, III, and IV, respectively), where **B** can be Arginine or Lysine, Ψ is a non-polar amino acid, and X is any amino acid, are multi-functional motifs that impart the capacity to bind nucleic acids and other proteins, i.e. receptors [21, 22, 24]. These motifs give LLPs a high affinity for GAGs, such as heparin and heparan sulfate. Binding of heparan sulfate proteoglycans (HSPG) may involve both GAG moieties and ligand-binding modules of the HSPG core protein [25].

In a previous report [5], we described structural similarities between Apo E and dengue capsid protein, PDB: 1LPE and 1R6R, respectively. Although their primary structures are not significantly similar, their secondary and tertiary structures are alike, i.e. helix-loop-helix; and, it has been confirmed experimentally that both proteins possess nucleic acid-binding and nuclear transit capacity [26, 27]. The Apo E receptor ligand motifs and receptor binding domain are well-established [28]; however, the exact cell entry “codes” have yet to be elucidated in Flavivirus envelope and capsid proteins.

Our present studies are based on the hypothesis that proteins of the LDL receptor gene family ubiquitously expressed in human and mosquito may be used by DENV for cell entry. Our goals were to identify potential receptor ligand motifs in dengue envelope and capsid proteins by sequence comparison to the motifs in Apo B100 and Apo E; use fluorescence-labeled synthetic peptides to assess cell binding/entry capacity of the viral proteins; and, assess effects of LDL and Apo E on binding and uptake of viral peptides using live HeLa cells in culture. Our findings may have implications for intervention strategies in viral infections in general.

METHODS

DENV polyprotein sequences used in this study were obtained from NIH NCBI PUBMED Protein and Structure databases.

Chemicals

Phosphate-buffered saline (PBS) and cell culture media were from Media Tech, Inc., Herndon, VA. Penicillin G-Sodium, streptomycin sulfate, Fetal Bovine Serum, Trypsin, Corning Costar 6 and 12 well culture plates, and 8 well Lab-Tek Chamber glass slides with cover were from Thermo Fisher Scientific, Inc. Mevastatin was from Sigma-Aldrich, Inc. Trypan Blue (modified) 0.4% solution in PBS was from MP Biomedicals, LLC, Solon, OH.

Fluorescence-labeled Peptides

Fluorescence-labeled synthetic peptides (Tables 1–3), of 95% or greater purity by HPLC analysis, were from NEO Group, Inc. Cambridge, MA. Peptides were received in lyophilized form in sealed 1 mL vials and solubilized in PBS-10 mM $MgCl_2$ to yield 1 mg/mL.

Protein Labeling

Purified human Apo E (> 95%), was from Athens Research & Technology, Athens GA. LDL was isolated as described previously [5] from pooled normal human plasma from Innovative Research, Inc., Movi, MI. For covalent labeling of the protein, 250 μL of ethanol was added to the vial containing 50 μg CM-DiI (7000), a thiol-reactive fluorescence compound from Invitrogen, Inc., to make a stock solution. Next, 1 μL of CM-DiI stock solution was added to 150 μg of Apo E in 500 μL or to 1 mg of purified LDL in 1 mL of PBS-5 mM $MgCl_2$. These reaction mixtures were allowed to stand for 30 minutes at ambient temperature then dialyzed in 1 liter PBS-$MgCl_2$ with three changes overnight.

Cells

HeLa cells (human cervix epithelial adenocarcinoma cell line, CCL-2™) were from American Type Culture Collection (ATCC). Typically, cells were stored in liquid Nitrogen until needed, then seeded and propagated according to ATCC protocols in DMEM supplemented with 10% FBS, 100 units Penicillin G-Sodium and 100 units/mL Streptomycin sulfate (DMEM – P/S -FBS) at 37°C in an atmosphere of 5% CO_2 in a humidified incubator. Cells at ~70% confluence were incubated overnight in DMEM – P/S – 3% FBS medium containing 40 μM Mevastatin, after which medium was replaced with 1 mL PBS. Labeled peptides (alone or with a potential competitor for receptor binding, Apo E, Apo E-derived peptide, or LDL) were added to each well then incubated under same conditions as above. Time-course and peptide concentration studies were conducted using FITC-labeled peptides to determine minimal concentration required to detect fluorescence signal, incubation period required for binding and/or uptake, and potential cytotoxicity. For Dsp2EP-FITC, 0.5–45 μg/mL of peptide (0.2 – 10.6 μM) was used, and the cells were observed for 5–120 min. Assays for Dsp3CP-FITC binding to HeLa cells were conducted using increasing concentrations of the peptide: 6.75 μM, 13.5 μM, 20.25 μM, 27 μM, 33.75 μM, 40.5 μM, and 47.25 μM. Cells were monitored at 15-minute intervals for 60 minutes and experiment was terminated at 90-minute time point.

To reduce background fluorescence the assay mixture was removed and live cells were rinsed thrice with PBS. In quenching experiments cells were incubated at ambient

temperature for 10 minutes using PBS with 0.2% Trypan Blue. Live cells were then rinsed with PBS sufficiently to visualize cells to obtain bright-light images as described below.

Dual Label Experiments

In these experiments, Dsp2EP-FITC was used in combination with either Apo E-CM-DiI or LDL-CM-DiI. Cells in 8 chamber slides were preconditioned as routine, rinsed with PBS-5 mM $MgCl_2$, incubated for 15 minutes at ambient temperature in 100 μL PBS-$MgCl_2$ containing 5 μg Dsp2EP-FITC mixed with 1.5 μg Apo E-CM-DiI or 5.0 μg LDL-CM-DiI. Binding assay mix was removed and cells rinsed in PBS prior to microscopy analysis in 200 μL PBS-$MgCl_2$. Images of live cells were obtained as before using green and red filters. Overlay images of Dsp2EP-FITC (green fluorescence image) and Apo E-CM-DiI or LDL-CM-DiI (red fluorescence image) were created using Adobe Photoshop CS 4 as described below. Representative regions showing signals green, red and yellow were enlarged and subjected to digital analysis using ImageJ. Color was split into channels red, blue and green, and raw integrated densities for each color were rendered in 3-D.

In similar experiments, 50 μg Dsp3CP-FITC was combined with 75 μg Apo E-CM-DiI in 300 μL PBS-MgCl2. Increasing volumes, 8, 16, 24, 32 and 40 μL, of this mixture were added to cells preconditioned as above in an 8-chamber slide in PBS-MgCl2 in 200 μL assay. These were then incubated at 37° C for 15 and 90 minutes.

Fluorescence Microscopy

All images were obtained using live cells in PBS-MgCl2 in culture trays or 8-well slides. Microscopy was performed using a Zeiss Axiovert 25 equipped with Zeiss objectives and FITC/GFP (Zeiss HQ470/40x and HQ525/50m) and red (Chroma AT540/25x and AT605/55m) filter cubes. Images were captured thru a 0.5x C-mount adapter using an Optronics Microfire CCD camera and Picture Frame software.

Adobe Photoshop CS Version 4 was used to enhance images. Full-frame images of field of view, equal in size and dimensions were used to create overlay images [5]. Analysis and assessment of raw integrated densities values were obtained using ImageJ, which was also used to render 3-D images.

RESULTS AND DISCUSSION

Results

Apo E binds all members of the LDL receptor super-family [19, 23, 29]. The receptor ligand sequence in Apo E spans residues ^{0130}Thr-Ala^{0159} [30, 31] and contains Type I and II ligand motifs, and both types of NLS sequences (Table 1). Apo E also contains two Type III motifs, at ^{071}Leu-Ser^{076} and ^{091}Ala-Glu^{096} and additional NLS (Table 1). Peptide E^{0131}-FITC, spanning Glu^{0131}-Gly^{0173}, contains the receptor ligand sequence L**RK**L**RK**RLL**R**. Synthetic peptides of the apo E LDLR ligand region have been used to substantiate a variety of functions for this apolipoprotein [31–33], including anti-infective activity [34–36]. Lysines in this sequence are essential in binding to the LDL B/E receptors [28]. Interaction of E^{0131}-FITC with HeLa cells was evaluated in the presence or absence of LDL. Figure 1

shows images obtained with E^{0131}-FITC (frame A and B) and E^{0131}-FITC plus highly purified human LDL (C and D). E^{0131}-FITC appears to bind to the cell surface (A) and form clusters (B) but does not appear to enter the cell. In contrast, the peptide signal is seen inside the cell when LDL is added to the assay (Frame C) as verified by quenching of fluorescence using Trypan Blue (not shown). Hence, synthetic peptides of the Apo E molecule retain cell binding properties of the intact molecule (not necessarily the capacity for internalization) and may be used to identify functional LDLR ligand motifs in DENV proteins.

The LDLR ligand motifs in Table 1 were used to identify sequences with similar function potential in DENV capsid and envelope proteins. The first 800 N-terminal residues of the DENV polyproteins include capsid (^{0001}Met – Arg^{0100}), precursor Membrane protein (^{0115}Phe – Thr^{0280}), and envelope glycoprotein E (^{0281}Met – Ala^{0775}) contain numerous potential receptor/GAG ligand motifs and NLS sequences (Tables 2 and 3).

Dengue Virus 2 Envelope Glycoprotein—Peptide Dsp2-EP with two ligand motifs, Ψ**B**Ψ**B**X, and one NLS sequence, X**B**X**B**X**B**X (Table 2), was evaluated for cell-binding capacity. A comparison of similar motifs present in Apo E and Apo B200 is included in Table 2. Only Type III ligand motifs are present in DENV envelope protein (E protein) sequences that are rich in Glycine, Lysine and Arginine residues, approximately 10%, 7% and 3%, respectively. Figure 2 images A1 – A4 show that Dsp2EP-FITC binds HeLa cells but doesn't appear in the cytoplasm. Images A2 and A4, enlarged areas of A1 and a similar field of view, clearly demonstrate the appearance of clusters on the cell surface. Mutated synthetic peptides Dsp2EP (B)- and (C)–FITC in which Aspartates replace basic residues in one of the ligand motifs (Table 2) also bind cells and do not appear in cytoplasm. Images A3, B3 and C3 show that addition of Trypan blue dye quenches fluorescence and confirms that Dsp2-EP and mutated forms bind to the cell surface but lack cell entry capacity. Raw Integrated Densities for images A1, B1, and C1 obtained using ImageJ are shown in Figure 2B. Reduced Integrated Densities are observed for the mutated peptides indicating that each ligand motifs may be functional but not as efficient in binding as their combination in Dsp2EP.

HeLa cells were used to test cell binding properties of Dsp2EP-FITC in presence of Apo E and LDL. Increasing amounts of unlabeled Apo E were included with 10 μg Dsp2EP-FITC in 500 μL PBS/5 mM MgCl2 and placed at 4°C for 18 hours. In parallel, unlabeled human LDL was added to HeLa cells and similarly incubated. Overlays of bright light and fluorescence images are shown in the lower section of Figure 3. Image A shows fluorescence obtained for 10 μg Dsp2EP-FITC (positive control). Images B and C were obtained with cultures containing 10 μg Dsp2EP-FITC in presence 400 μg of unlabeled Apo E (B) and 300 μg of unlabeled LDL (C) in the assay. Enlarged areas in A1, B1 and C1, respectively, show that fluorescence appears both diffused on the cell surface and in clusters.

Graph 1 in Figure 3B shows the number of loci of Dsp2-EP-FITC bound to HeLa cells in presence of unlabeled Apo E-2 peptide and LDL (10 μg of the peptide in all wells; effects of 40 μg, 160 μg, 400 μg of Apo E-2, and 300 μg, 600 μg, 1200 μg of LDL). Addition of unlabeled Apo E-2 peptide enhances Dsp2EP binding significantly as is shown by the increase in the number of loci with fluorescence (Graph B, blue columns) and the increase in

total Raw Integrated Density (Graph 3C, blue columns). Also, results in image Figure 3B indicates that addition of Apo E-2 makes receptors available almost ubiquitously across the field of view. In comparison, the presence of LDL reduce the number of Dsp2EP-FITC fluorescing loci as shown in image C and graph B (orange columns). These data also indicate that receptors for the Dsp2EP-FITC are made available in a limited number of cells. Our observations suggest a mechanism in which increased concentration of Apo E-2 triggers a conformational change in the receptor making more binding modules available for Dsp2EP-FITC binding, a mechanism reported previously for LDL receptors [23, 37, 38].

Dual label experiments using Dsp2EP-FITC with either Apo E-CM-DiI or LDL-CM-DiI, as described in Methods, were performed to assess colocalization of Dsp2EP-FITC with Apo E and LDL. Images were obtained as described above. Overlay in frame A of Figure 4 shows combined fluorescence of Dsp2EP-FITC and Apo E-CM-DiI. Enlarged representative regions showing green, red and yellow signals are indicated by 1 – 8. Each image was subjected to digital analysis using ImageJ and split into channels red, blue and green, and raw integrated densities were then rendered in 3-D. Enlarged images 1, 2, 5 and 6 are shown at bottom two rows of Figure 4 as 1G, 1R, etc. 3-D images reveal that Dsp2EP-FITC binds solo as well as colocalized within the red clusters formed by Apo E-CM-DiI. These observations suggest that Dsp2EP-FITC and Apo E-CM-DiI may share receptors, binding to either the same or adjacent receptor molecules. Apo E-CM-DiI signal appears uniformly in clusters with similar maxima in all enlarged images, 1R, 2R, 5R and 6R, in Figure 4. This may indicate saturation in the area density of receptors occupied by Apo E, which is consistent with the finding that each LDLR provides two modules for Apo E binding [38]. This mechanism may leave sufficient number of unoccupied modules for binding to other ligands, such as Dsp2EP-FITC.

Results of parallel dual label experiments using Dsp2EP-FITC and LDL-CM-DiI are shown in Figure 5. A section of an overlay image presented in frame A shows separate loci of LDL-CM-DiI and Dsp2EP-FITC, respectively, while a yellow signal indicates co-location. Areas 1, 2 and 3 in Frame A are shown enlarged as images 1, 2 and 3 in the row beneath. Image 1 shows loci of Dsp2EP-FITC alone and collocated with LDL-CM-DiI, as pinkish and yellow signals (also evident in 1G and 1R). Image 2 shows loci indicating LDL-CM-DiI predominantly (2R) except for two green dots identified as Dsp2EP-FITC (2G). Image 3 suggests a stronger presence of Dsp2EP-FITC versus LDL-CM-DiI that is supported by 3R and 3G. LDL-CM-DiI appears to form clusters similar to those seen for Apo E-CM-DiI discussed above. These results suggest that in some regions of the cell surface Dsp2EP-FITC may interact with the same receptor molecules as do Apo E and LDL.

Dengue Virus 3 Capsid Protein—The DENV nucleocapsid, encasing the viral genome, is enclosed by the bilayer lipid membrane in which the envelope glycoprotein is anchored [1]. The nucleocapsid is comprised of multiple molecules of the capsid protein (C protein) associated with lipid. In DENV capsid proteins (residues 0001 – 0100 of the viral polyprotein), basic amino acids K and R represent approximately 26% of the sequence and are present in approximately equimolar concentrations. Ligand motifs, I, II, and III, are abundant (Table 3) and may impart the capsid protein with multiple options in binding to both receptor proteins and glycosaminoglycans. Such binding capacities may be functionally

significant (see Discussion). Type I ligand motifs are present in DENV1, 3, and 4 C proteins, motif Types II and III occur in the capsids of all four viral versions; there is also a surplus of potential mono- and bipartite NLS.

Dsp3CP-FITC (^{0002}Asn-Gln^{0028} of the DENV3 capsid protein, Table 3), contains a type I, Q**RKK**TG**K**P, and a type II, L**KR**V**R**NR motifs (Table 3), that may function as mono- and as components of a bipartite NLS. Dsp3CP-FITC was tested for cell entry and nuclear translocation potential in mevastatin-treated HeLa cells. Results are shown in Figure 6, A1 and A2 (an enlarged area of A1). Fluorescence appears located in cytoplasm in apparent endosomes, and clusters are seen in the nuclear space. This distribution of fluorescence is seen in most images obtained with Dsp3CP-FITC. Similar patterns were observed in presence of increasing concentrations of unlabeled Apo E-2. Examples are shown in Figure 6 B1, with an enlarged area in B2, which shows Dsp3CP-FITC signal in loci suggesting endosomes, at loci proximal to the nuclear envelope, and possibly in the nuclear space. Hence, apo E-2 peptide at 1.5 molar excess does not appear to influence cell entry or nuclear translocation of Dsp3CP-FITC.

In dual label experiments, Apo E-CM-DiI was added with Dsp3CP-FITC to live HeLa cells in FBS-depleted EMEM then incubated at ambient temperature for 15 and 90 minutes. Results are shown as overlays in Figure 6 rows C and D, respectively. At 15 minutes (row C), colocalized signals are evident across the field of view with most appearing at the cell surface. This observation suggests a sharing of receptors and/or clustering of receptors carrying different signals. Enlarged overlay C1 shows a cell with colocalized signals at the membrane, in the cytoplasmic space, and apparently in the nuclear space. Enlarged overlays C2 and C3 show colocalized signals at discrete loci on cell surface. Dsp3CP-FITC represents ~71% raw integrated density; this includes diffused green, whitish green clusters indicating colocalized signals in the cytoplasm, and possibly in the nuclei. At the 90 minute point (row D), intracellular separation of Dsp3CP-FITC and Apo E-CM-DiI is evident. Dsp3CP-FITC signal appears both at discrete loci and diffused in cytoplasm. Elevated green fluorescence background may indicate binding of Dsp3CP-FITC to extracellular debris on culture plate. In overlays D1 – D3 Apo E-CM-DiI is clearly separated from the diffused Dsp3CP-FITC; red signal seems to fill the nuclear space, where colocalization of the two signals is also apparent (yellow dots). These results *in toto* suggest Dsp3CP-FITC, which contains receptors ligand motifs and NLS sequences, may share LDL B/E receptors in cell entry, then translocate to nucleus.

Discussion

Humans, sylvatic non-human primates, and mosquitoes are major reservoirs of DENV and other *Flaviviridae* [39]. LDLR and/or LRPs are expressed in most cell types in humans. Analogues proteins in *Aedes aegypti* [40–42] and *Culex quinquefasciatus* [43] include apolipophorins and lipophorin receptor [44–47]. There are 17 different known members in the LDL receptor gene family (LRPs) including LDLR, VLDLR, LRPs 1–6, 8, 10, 11, and 12, Megalin (LRP2), and ST7p. All members have five distinct structural components, three are extracellular, 1 transmembrane sequence, and a cytoplasmic, carboxyl region [48]. Relevant to the present report are the numerous clusters of ligand-binding, cysteine-rich

modules contained in the extracellular domain (also known as complement-like repeats and ligand adhesion type A units). There are a total of 170 known renditions of ligand-binding modules that recognize at least 30 different ligands belonging to a variety of protein families. All LRPs are thought to bind apo E [48].

DENVs are known to employ multiple mechanisms to obtain cell entry [11, 49]. There is evidence that DENV interacts initially with heparan sulfate proteoglycans essential in anchoring at the cell surface [50, 51]. Several target proteins on the cell surface have been identified and clathrin-mediated endocytosis has been shown to play role in DENV internalization in both mammalian and insect cells [49, 52–54]. It is possible that viruses have evolved to use abundant LDL and LRP receptors to gain ubiquitous access to human tissues. These receptors provide classical examples for the cargo internalization via clathrin-mediated endocytosis; they are also glycosylated, hence may provide GAG-mediated initial attachment of the virion which facilitates specific interaction with the receptor.

DENVs are known to infect a variety of tissues [55] *in vivo* and numerous human cell types *in vitro* including epithelial cells [56] and HeLa cells [57]. Dendritic cells (DCs) and macrophages are the primary targets for DENV infection in human blood [58, 59]. Permissive monocytes, antigen presenting cells, ingest and process the viral particle prior to presenting its components, proteins and nucleic acid, to immune response cells, T-cells, in the lymph nodes [60, 61]. In DCs, dengue viruses are recognized by a C-type lectin, DC-specific intercellular adhesion molecule-3 grabbing non-integrin (DC-SIGN) [58, 59]. DC-SIGN also recognizes the arenavirus Lassa virus [62], and the Enterovirus 71 [63].

When the mosquito injects its beveled stinger (proboscis) into the epidermis it deposits a mixture of salivary proteins along with the DENV particles. Keratinocytes that can express the LDLR [64] and LRP1a [65] and make up 95% of the epidermis may represent the first line of defense against arboviruses. Only a small fraction of the DENV injected by the mosquito enters the blood compartment and is addressed by the dendritic cells [60]. The rest may remain with the tissues at the injection site where the keratinocytes stimulate inflammation and activate Langerhans cells [66]. By comparison, only chemically modified forms of LDL, e.g. oxidized-LDL, are engulfed and removed from the blood by DC-scavenger receptors [67]; native LDL is removed from circulation by various tissues expressing LDLR and LRPs.

The hypothesis of DENV specific interaction to LDL or related receptor is strongly supported by sequence comparison of viral proteins to known LDLR/LRP ligands. In the Apo E receptor ligand site (^{0130}Thr-Ala^{0159}; PDB: 1LPE), Lysine residues in positions 0143 and 0146, 0141L**R**<u>**K**</u>L**R**<u>**K**</u>**R**LL**R**^{0150} are essential for binding LDL B/E receptors [28] and Arginine residues located between ^{0170}Ala-Leu^{0181} are involved in binding GAGs and Heparan Sulfate Proteoglycans, HSPGs [24]. Our examination of the DENV polyprotein sequences revealed that potential ligand analogues occur in structural as well as in non-structural proteins. In DENV, the envelope glycoproteins that span residues ^{0281}Met-Ala^{0775} make the initial contact with receptor molecules on the cell surface [68]. We posited that this interaction involves the LDLR Lysine/Arginine-rich ligand motifs contained in the DENV envelope and capsid proteins.

In DENV envelope proteins, the region essential for cell entry, Domain III, spans ^{0580}Ser-Trp^{0671} [69]. Studies by Falconar [70] showed that a neutralizing monoclonal 3A8.1 has a high binding avidity for several DENV2 E protein-derived peptides, including ^{0568}**R**MD**K**LQLKG^{0576} and ^{0584}GKF**K**IV**K**EI^{0592} located in E protein Domains I and III, respectively [71]. Both peptides contain LDLR Type III ligand motifs (Table 1); analogues are present as ^{0567}L**K**MD**K**L in DENV1 and 3, as ^{0567}L/V**R**MD/E**K**L^{0572} in DENV2 and DENV4, and as ^{0586}F**K**LE/V**K**E^{0591} in DENV1 and 2 (Table 4). The latter motif is absent in DENV3 and 4. Instead, DENV4 E protein has an analogue of the motif as ^{0478}LM**K**MK**K**KT^{0485}. In the PBD model 1OAN of the DENV2, both motifs in tandem appear in a loop located on the surface of the molecule.

We used fluorescence labeled synthetic peptides of DENV sequences containing LDLR/LRP ligand motifs in dual label experiments with apo E CM-DiI and LDL CM-DiI. This approach presents advantages over using an intact virus including cost issues, safety issues, and steric hindrance. As illustrated in the Results, our Dsp2EP-FITC peptide that spans DENV2 region ^{0564}Lys-^{0595} and contains the two Type III ligand motifs, binds HeLa cells but is not internalized. Dsp2EP-FITC also binds HepG2 cells (shown as a Supplemental Figure 1). Dsp2EP-FITC (B) and (C), mutated forms of Dsp2EP-FITC, bind HeLa cells with lower integrated density (Fig. 2B). Similar binding pattern (decreased binding of the mutated peptides compared to the non-modified version) was observed with dextran sulfate cellulose beads (Supplemental Figure 2). These results confirm that residues Arg^{0568}, Lys^{0571}, Lys^{0587} and Lys^{0590} in LDLR ligand motifs play a role in binding to the cell surface. Colocalization of Apo E-CM-DiI and Dsp2EP-FITC suggests that they may bind the same receptor or adjacent molecules. The LDL receptor contains 7 copies of the ligand modules, and Apo E binds only LA4 and 5 modules [38]. Hence, presence of Apo E-FITC may not hinder binding of Dsp2EP-FITC to the remaining modules, and would result in colocalized red and green signals. Further, involvement of other LRPs should not be ruled out.

Sequence similarities exhibited by human Apo E, Apo B, and DENV capsid proteins were first described in our earlier report [5]. The 3-D models of Apo E [27] and DENV2 capsid protein [26] show that both are helix-loop/turn-helix molecules with amphipathic features that encourage homodimerization in a pure state and perhaps heterodimerization in a mixture. These common properties may account for DENV capsid protein specific interaction with VLDL [72]. All three proteins associate with lipids, bind nucleic acids, possess cell entry capacity and translocate to the cell nucleus.

The primary structures of DENV capsid proteins suggest them to be multi-functional proteins with analogues of LDLR and LRP ligand and NLS motifs at both termini [73, 74]. Based on our studies, DENV3 capsid may have inherent cell entry capacity. LRP ligand analogues occur within the first 40 residues of the N-termini of DENV capsid proteins. In DENV3 capsid protein two ligand motifs, RKKTGK and LKRVRN, two mono-NLS (^{0005}Arg-Lys^{0010}, ^{0017}Lys-Arg^{0020}), and one bi-NLS (^{0006}Lys-Arg^{0020}) motifs likely provide the capsid not only with cell entry capacity but also with potential to transit into the nucleus. DENV2 C protein the Type II ligand analogue, ^{0004}QR**K**KA**K**N^{0010}, is also a high affinity LRP ligand. DENV1 and 4 C proteins, ^{0004}Q**RKK**TG**R**P^{0011} and ^{0003}Q**RKK**VV**R**P^{0010}, respectively, are Type I ligand motifs and may impart both LRP/GAG binding and nuclear

translocation potentials. Our results and those reported by others [75] support the premise that the intact DENV capsids have inherent infectivity capacity and may be an important player in the second phase of the DENV infection process as an unfinished/immature viral particle.

Considering that LDLR/LRP receptors occur ubiquitously in humans, sylvatic mammals, and mosquitoes, *Aedes sp.* and *Culex sp.*, and that the receptor ligand motifs are mimicked by DENVs [76], it is possible that DENV possesses a “pass” into virtually any human cell type. Then vascular leakage of the virus in DHF syndrome [77] could lead to infection of vital organs such as liver, spleen, lungs, heart, and kidneys. High level of infectivity provided by the LDLR/LRP mechanism may be a major factor in dengue shock syndrome and dengue hemorrhagic fever.

CONCLUSION

We conclude that dengue viruses may have the capacity to achieve cell binding and entry via the receptors utilized by low-density lipoproteins. Our results indicate that dengue capsid and envelope proteins contain Lysine-based LDL receptor ligand and NLS motifs. Synthetic peptides of DENV proteins, representing potential LDL receptor binding sites, colocalize with LDL and apo E on the cell surface. In humans and other mammals LDL receptors are expressed ubiquitously throughout the organism, a factor that may greatly enhance viral infectivity. The processes for cell entry for dengue virus have not been fully elaborated, and our report provides an additional intriguing possibility for molecular mechanisms of viral entry.

Supplementary Material

Refer to Web version on PubMed Central for supplementary material.

Acknowledgments

Studies were supported in part by grants F49620-99-1-0327 (AFOSR, PI – J. Guevara), FA 9550-05-1-0472 (AFOSR, PI – A. Hanke), SC2GM081218 and SC3GM099637 (NIH, PI – N. Guevara). Mr. Troy McWhorter donated his time and effort on this project. Mr. Jaime Romo, Jr., was supported by R25GM083755 (NIH, PIs – J. Facelli, S. Nair).

ABBREVIATIONS

CP	C protein capsid protein
Cm-DiI	Cell Tracker C7000
DENV	dengue virus
FITC	Fluorescein Isothiocyanate
GAGs	glycosaminoglycans
HSPG	heparin sulfate proteoglycan
IDL	intermediate density lipoprotein

LDL	low density lipoprotein
LDLR	low density lipoprotein receptor
LLP(s)	low density lipoprotein particle(s)
NLS	nuclear localization signal
VLDL	very low density lipoprotein

References

1. Kuhn RJ, Zhang W, Rossmann MG, Pletnev SV, Corver J, et al. Structure of dengue virus: implications for flavivirus organization, maturation, and fusion. Cell. 2002; 108:717–725. [PubMed: 11893341]
2. Orlova EV, Sherman MB, Chiu W, Mowri H, Smith LC, et al. Three-dimensional structure of low density lipoproteins by electron cryomicroscopy. Proc Natl Acad Sci USA. 1999; 96:8420–8425. [PubMed: 10411890]
3. Scanu AM, Wisdom C. Serum lipoproteins structure and function. Annu Rev Biochem. 1972; 41:703–730. [PubMed: 4343457]
4. Lindenbach, BD.; Thiel, H-J.; Rice, CM. Flaviviridae: The Viruses and Their Replication. In: Knipe, DM.; Howley, PM., editors. Fields Virology. Philadelphia: Lippincott, Williams, Wilkins; 2006. p. 1101-1152.Chapter 33
5. Guevara J Jr, Prashad N, Ermolinsky B, Gaubatz JW, Kang D, et al. Apo B100 similarities to viral proteins suggest basis for LDL-DNA binding and transfection capacity. J Lipid Res. 2010; 51:1704–1718. [PubMed: 20173184]
6. Gubler, DJ.; Kuno, G.; Markoff, L. Flaviviruses. In: Knipe, DM.; Howley, PM., editors. Fields Virology. Philadelphia: Lippincott, Williams, Wilkins; 2006. p. 1153-1252.Chapter 34
7. Gould EA, Solomon T. Pathogenic flaviviruses. Lancet. 2008; 371:500–509. [PubMed: 18262042]
8. Fischl W, Bartenschlager R. Exploitation of cellular pathways by Dengue virus. Curr Opin Microbiol. 2011; 14:470–475. [PubMed: 21798792]
9. Mukhopadhyay S, Kuhn RJ, Rossmann MG. A structural perspective of the Flavivirus life cycle. Nat Rev Microbiol. 2005; 3:13–22. [PubMed: 15608696]
10. Mosso C, Galvan-Mendoza IJ, Ludert JE, del Angel RM. Endocytic pathway followed by dengue virus to infect the mosquito cell line C6/36 HT. Virology. 2008; 378:193–199. [PubMed: 18571214]
11. Mercer J, Schelhaas M, Helenius A. Virus entry by endocytosis. Ann Rev Biochem. 2010; 79:803–833. [PubMed: 20196649]
12. van der Schaar HM, Rust MJ, Chen C, van der Ende-Metselaar H, Wilschut J, et al. Dissecting the cell entry pathway of dengue virus by single-particle tracking in living cells. PLoS Pathog. 2008; 4(12) Article ID e1000244.
13. Halstead SB, Heinz FX, Barrett ADT, Roehrig JT. “Dengue virus: molecular basis of cell entry and pathogenesis”, 25–27 June 2003, Vienna, Austria. Vaccine. 2005; 23:849–856. [PubMed: 15603884]
14. Crill WD, Roehrig JT. Monoclonal antibodies that bind to domain III of Dengue virus E glycoprotein are the most efficient blockers of virus adsorption to Vero cells. J Virol. 2001; 75:7769–7773. [PubMed: 11462053]
15. Karlsson H, Leanderson P, Tagesson C, Lindahl M. Lipoproteomics I: Mapping proteins in low-density lipoprotein using two-dimensional gel electrophoresis and mass spectrometry. Proteomics. 2005; 5:551–565. [PubMed: 15627967]
16. Sun H-Y, Chen S-F, Lai M-D, Chang T-T, Chen T-L, et al. Comparative proteomic profiling of plasma very-low-density and low-density lipoproteins. Clin Chim Acta. 2010; 411:336–344. [PubMed: 19945452]

17. Callow J, Summers LKM, Bradshaw H, Frayn KN. Changes in LDL particle composition after the consumption of meals containing different amounts and types of fat. Am J Clin Nutr. 2002; 76:345–350. [PubMed: 12145005]
18. Prassl R. Human low density lipoprotein: the mystery of core lipid packing. J Lipid Res. 2011; 52:187–188. [PubMed: 21131533]
19. Goldstein JL, Brown MS. History of Discovery: The LDL Receptor. Arterioscler Thromb Vasc Biol. 2009; 29:431–438. [PubMed: 19299327]
20. Dyer CA, Cistola DP, Parry GC, Curtiss LK. Structural features of synthetic peptides of apolipoprotein E that bind the LDL receptor. J Lipid Res. 1995; 36:80–88. [PubMed: 7706950]
21. Yang CY, Chen SH, Gianturco SH, Bradley WA, Sparrow JT, et al. Sequence, structure, receptor-binding domains and internal repeats of human apolipoprotein B-100. Nature. 1986; 323:738–742. [PubMed: 3095664]
22. Hospattankar AV, Law SW, Lackner K, Brewer HB Jr. Identification of low density lipoprotein receptor binding domains of human apolipoprotein B-100: a proposed consensus LDL receptor binding sequence of apo B-100. Biochem Biophys Res Comm. 1986; 139:1078–1085. [PubMed: 3767991]
23. Guttman M, Prieto PH, Croy JE, Komives EA. Decoding of lipoprotein-receptor interactions: properties of ligand binding modules governing interactions with apolipoprotein E. Biochemistry. 2010; 49:1207–1216. [PubMed: 20030366]
24. Cardin AD, Weintraub HJ. Molecular modeling of protein-glycosaminoglycan interactions. Arterioscler Thromb Vasc Biol. 1989; 9:21–32.
25. Murdoch AD, Dodge GR, Cohen I, Tuan RS, Iozzo RV. Primary structure of the human heparan sulfate proteoglycan from basement membrane (HSPG2/perlecan). A chimeric molecule with multiple domains homologous to the low density lipoprotein receptor, laminin, neural cell adhesion molecules, and epidermal growth factor. J Biol Chem. 1992; 267:8544–8557. [PubMed: 1569102]
26. Ma L, Jones CT, Groesch TC, Kuhn RJ, Post CB. Solution structure of dengue virus capsid protein reveals another fold. Proc Nat Acad Sci USA. 2004; 101:3414–3419. [PubMed: 14993605]
27. Wilson C, Wardell MR, Weisgraber KH, Mahley RW, Agard DA. Three-dimensional structure of the LDL receptor-binding domain of human apolipoprotein E. Science. 1991; 252:1817–1822. [PubMed: 2063194]
28. Zaiou M, Arnold KS, Newhouse YM, Innerarity TL, Weisgraber KH, et al. Apolipoprotein E-low density lipoprotein receptor interaction: influences of basic residue and amphipathic α-helix organization in the ligand. J Lipid Res. 2000; 41:1087–1095. [PubMed: 10884290]
29. Guttman M, Prieto JH, Handel TM, Domaille PJ, Komives EA. Structure of the minimal interface between ApoE and LRP. J Mol Biol. 2010; 398:306–319. [PubMed: 20303980]
30. Dyer CA, Curtiss LK. A synthetic peptide mimic of plasma apolipoprotein E that binds the LDL receptor. J Biol Chem. 1991; 266:22803–22806. [PubMed: 1744074]
31. Nikoulin IR, Curtiss LK. An apolipoprotein E synthetic peptide targets to lipoproteins in plasma and mediates both cellular and lipoprotein interactions in vitro and acute clearance of cholesterol-rich lipoproteins in Vivo. J Clin Invest. 1998; 101:223–234. [PubMed: 9421485]
32. Hsieh Y-H, Chou C-Y. Structural and functional characterization of human apolipoprotein E 72–166 peptides in both aqueous and lipid environments. J BioMed Sci. 2011; 18:4. [PubMed: 21219628]
33. Christensen DJ, Ohkubo N, Oddo J, Van Kanegan MJ, Neil J, et al. Apolipoprotein E and peptide mimetics module inflammation by binding the SET protein and activating protein phosphatase 2A. J Immunol. 2011; 186:2535–2542. [PubMed: 21289314]
34. Dobson CB, Sales SD, Hoggard P, Wozniak MA, Crutcher KA. The receptor-binding region of human apolipoprotein E has direct anti-infective activity. J Infect Diseases. 2006; 193:442–450. [PubMed: 16388493]
35. Liu S, McCormick KD, Zhao W, Zhao T, Fan D, et al. Human apolipoprotein E peptides inhibit hepatitis C virus entry by blocking virus binding. Hepatology. 2012; 56:484–491. [PubMed: 22334503]

36. Kelly BA, Neil SJ, McKnight A, Santos JM, Sinnis P, et al. Apolipoprotein E-derived antimicrobial peptide analogues with altered membrane affinity and increased potency and breadth of activity. FEBS J. 2007; 274:4511–4525. [PubMed: 17681018]
37. Beglova N, Jeon H, Fisher C, Blacklow SC. Structural features of the low-density lipoprotein receptor facilitating ligand binding and release. Biochem Soc Trans. 2004; 32:721–723. [PubMed: 15493997]
38. Fisher C, Abdul-Aziz D, Blacklow SC. A two-module region of the low-density lipoprotein receptor sufficient for formation of complexes with apolipoprotein E ligands. Biochemistry. 2004; 43:1037–1044. [PubMed: 14744149]
39. Gould EA, Solomon T. Pathogenic Flaviviruses. Lancet. 2008; 371:500–509. [PubMed: 18262042]
40. Roosendaal SD, Van Doorn JM, Valentijn KM, Van der Horst DJ, Rodenbury KW. Delipidation of insect lipoprotein, lipophorin, affects its binding to the lipophorin receptor, LpR: Implications for the role of LpR-mediated endocytosis. Insect Bioch Mol Biol. 2009; 30:135–144.
41. Cheon HM, Shin SW, Bian G, Park JH, Raikhel AS. Regulation of lipid metabolism genes, lipid carrier protein lipophorin, and its receptor during immune challenge in the mosquito Aedes aegypti. J Biol Chem. 2006; 281:8426–8435. [PubMed: 16449228]
42. Rodenburg KW, Van der Horst DJ. Review. Lipoprotein-mediated lipid transport in insects: analogy to the mammalian lipid carrier system and novel concepts for the functioning of LDL receptor family members. Bioch Biophys Acta. 2005; 1736:10–29.
43. Atkinson PW, Hemingway J, Christensen BM, Higgs S, Kodira C, et al. Annotation of Culex pipiens quinquefasciatus. 2009 Accession: XP_001864948.
44. van Heusden MC, Thompson F, Dennis J. Biosynthetic of Aedes aegyti lipophorin and gene expression of its apolipoproteins. Insect Bioch Mol Biol. 1998; 28:733–738.
45. Cheon H-M, Seo S-J, Sun J, Sappinton TW, Raikhel AS. Molecular characterization of the VLDL receptor homolog mediating binding of lipophorin in oocyte of the mosquito Aedes aegypti. Insect Bioch Mol Biol. 2001; 31:753–760.
46. Sappington TW, Raikhel AS. Ligand-binding domains in vitellogenin receptors and other LDL-receptor family members share a common ancestral ordering of cysteine-rich repeats. J Mol Evol. 1998; 46:476–487. [PubMed: 9541543]
47. Kumar BA, Paily KP. Up-regulation of lipophorin (Lp) and lipophorin receptor (LpR) gene in the mosquito, *Culex quinquefasciatus* (Diptera: Culicidae), infected with the filarial parasite, *Wuchereria bancrofti* (Spirurida: Onchocercidae). Parasitol Res. 2011; 108:377–381. [PubMed: 20922426]
48. Rebeck GW, LaDu MJ, Estus S, Bu G, Weeber EJ. Review. The generation and function of soluble apo E receptors in the CNS. Mol Neurodegen. 2006; 1:1–13.
49. Smit JM, Moesker B, Rodenhuis-Zybert I, Wilschut J. Flavivirus cell entry and membrane fusion. Viruses. 2011; 3(2):160–171. [PubMed: 22049308]
50. Chen Y, Maguire T, Hileman RE, Fromm JR, Esko JD. Dengue virus infectivity depends on envelope protein binding to target cell heparan sulfate. Nature. 1997; 3:866–871.
51. Watterson D, Kobe B, Young PR. Residues in domain III of the dengue virus envelope glycoprotein involved in cell-surface glycosaminoglycan binding. J Gen Virol. 2012; 93:72–82. [PubMed: 21957126]
52. Cabrera-Hernandez A, Smith DR. Mammalian dengue virus receptors. Dengue Bull. 2005; 29:119–135.
53. Reyes-del Valle J, Salas-Benito J, Soto-Acosta R, del Angel RM. Dengue virus cellular receptors and tropism. Curr Trop Med Rep. 2014; 1:36–43.
54. Paingankar MS, Gokhale MD, Deobagkar DN. Dengue-2-virus-interacting polypeptides involved in mosquito cell infection. Arch Virol. 2010; 155:1453–1461. [PubMed: 20571839]
55. Jessie K, Fong MY, Devi S, Lam SK, Wong KT. Localization of dengue virus in naturally infected human tissues, by immunohistochemistry and in situ hybridization. J Infect Dis. 2004; 189:1411–1418. [PubMed: 15073678]
56. Diamond MS, Edgil D, Roberts TG, Lu B, Harris E. Infection of human cells by dengue virus is modulated by different cell types and viral strains. J Virol. 2000; 74:7814–7823. [PubMed: 10933688]

57. Krishnan MN, Sukumaran B, Pal U, Agaisse H, Murray JL. Rab 5 is required for the cellular entry of dengue and West Nile viruses. J Virol. 2007; 81:4881–4885. [PubMed: 17301152]
58. Lozach P-Y, Burleigh L, Staropoli I, Navarro-Sanchez E, Harriague J. Dendritic cell-specific intercellular adhesion molecule 3-grabbing non-integrin (DC-SIGN)-mediated enhancement of dengue virus infection is independent of DC-SIGN internalization signals. J Biol Chem. 2005; 289:23698–23708. 2005. [PubMed: 15855154]
59. Tassaneetrithep B, Burgess TH, Granelli-Piperno A, Trumpfheller C, Finke J, et al. DC-SIGN (CD209) mediates dengue virus infection of human dendritic cells. J Exp Med. 2003; 197:823–829. [PubMed: 12682107]
60. Noisakran S, Onlamoon N, Songprakhon P, Hsiao H-M, Chokephaibulkit K, et al. Cells in dengue virus infection in vivo. Adv Virol. 2010 Article ID 164878.
61. Kwan W-H, Navarro-Sanchez E, Dumortier H, Decossas M, Vachon H, et al. Dermal-type macrophages expressing CD209/DC-SIGN show inherent resistance to dengue virus growth. PLoS NTD. 2008; 2(10) Article ID e311.
62. Goncalves A-R, Moraz M-L, Pasquato A, Helenius A, Lozach P-Y, et al. Role of DC-SIGN in Lassa virus entry into human dendritic cells. J Virol. 2013; 87:11504–11515. [PubMed: 23966408]
63. Ren X-X, Ma L, Liu Q-W, Li C, Huang Z, et al. The molecule of DC-SIGN captures enterovirus 71 and confers dendritic cell-mediated viral trans-infection. Virol J. 2014; 11:47. [PubMed: 24620896]
64. Williams ML, Mommaas-Keinhuis A-M, Rutherford SL, Grayson S, Vermeer BJ, et al. Free sterol metabolism and low density lipoprotein receptor expression as differentiation markers of cultured human keratinocytes. J Cell Physiol. 1987; 132:428–440. [PubMed: 2443512]
65. Galliano M-F, Toulza E, Jonca N, Gonias SL, Serre G, et al. Binding of α2ML1 to the low density lipoprotein receptor-related protein 1 (LRP1) reveals a new role for LRP1 in the human epidermis. PLoS ONE. 2008; 3(7) Article ID E-2729.
66. Barker JNWN, Mitra RS, Griffiths CEM, Dixit VM, Nickoloff BJ. Keratinocytes as initiators of inflammation. Lancet. 1991; 337:211–214. [PubMed: 1670850]
67. Nickel T, Schmauss D, Hanssen H, Sicic Z, Krebs B, et al. oxLDL uptake by dendritic cells induces up regulation of scavenger-receptors, maturation and differentiation. Atherosclerosis. 2009; 205:442–450. [PubMed: 19203752]
68. Chen Y, Maguire T, Marks RM. Demonstration of binding of dengue virus envelope protein by target cells. J Virol. 1996; 70:8765–8772. [PubMed: 8971005]
69. Erb SM, Butrapet S, Moss KJ, Luy BE, Childers T, et al. Domain-III FG loop of the dengue virus type 2 envelope protein is important for infection of mammalian cells and *Aedes aegypti* mosquitoes. Virology. 2010; 406:328–335. [PubMed: 20708768]
70. Falconar AKI. Use of synthetic peptides to represent surface-exposed epitopes defined by neutralizing dengue complex- and Flavivirus group-reactive monoclonal antibodies on the native dengue type-2 virus envelope glycoprotein. J Gen Virol. 2008; 89:1616–1621. [PubMed: 18559931]
71. Megret F, Hugnot JP, Falconar A, Gentry MK, Moren DM, et al. Use of recombinant fusion proteins and monoclonal antibodies to define linear and discontinuous antigenic sites on the dengue virus envelope glycoprotein. Virology. 1992; 187:480–491. [PubMed: 1372140]
72. Faustino AF, Carvalho FA, Martins IC, Castanho MA, Mohana-Borges R, et al. Dengue virus capsid protein interacts specifically with very low-density lipoproteins. Nanomedicine. 2014; 10:247–255. [PubMed: 23792329]
73. Wang S-H, Syu W-J, Huang K-J, Lei H-Y, Yao C-W, et al. Intracellular localization and determination of a nuclear localization signal of the core protein of dengue virus. J Gen Virol. 2002; 83:3093–3102. [PubMed: 12466486]
74. Samsa MM, Mondotte JA, Iglesias NG, Assunção-Miranda, Barbosa-Lima G, et al. Dengue virus capsid protein usurps lipid droplets for viral particle formation",. *PLoS Pathogens*, vol. 2009; 5(10) Article ID e1000632.
75. Balinsky CA, Schmeisser H, Ganesan S, Singh K, Pierson TC, et al. Nucleolin Interacts with the Dengue Virus Capsid Protein and Plays a Role in Formation of Infectious Virus Particles. J Virol. 2013; 87:13094–13106. [PubMed: 24027323]

76. Lin Y-S, Yeh T-M, Lin C-F, Wan S-W, Chuang Y-C, et al. Molecular mimicry between virus and host and its implications for dengue disease pathogenesis. Exp Biol Med. 2011; 236:515–523.

77. Trung, DT.; Wills, B. Systemic vascular leakage associated with dengue infections – The Clinical Perspective. In: Rothman, AL., editor. Dengue Virus Curr Topics Microbiol Immunol. Vol. 338. Springer-Verlag; Berlin Heidelberg: 2010. p. 57-66.

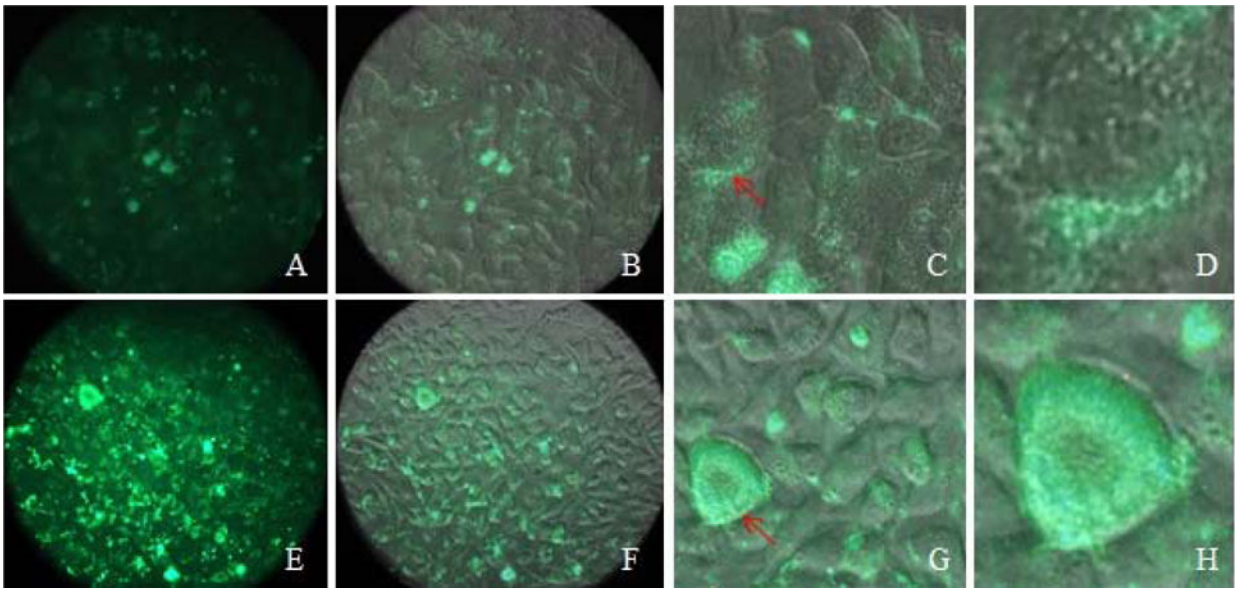

Figure 1. Influence of LDL on uptake of E^{0131}-FITC by HeLa cells

An assay solution of 5 μM E^{0131}-FITC in PBS containing 5 mM $MgCl_2$ was added to HeLa cells after cultures were preconditioned overnight in medium with 3% FBS and 1 μM Mevastatin and rinsed with PBS-$MgCl_2$. In parallel, 100 μg human LDL was added to mixture. Cells were incubated for 60 minutes. Fluorescence image A shows binding of E^{0131}-FITC to HeLa cells. An overlay image of frame A on the corresponding bright light image is shown in frame B. Images in frames C and D are enlargements of an area in B and show E^{0131}-FITC as clusters on the cell surface. Binding of E^{0131}-FITC in the presence of unlabeled LDL is shown in frame E with the corresponding overlay in frame F. Images in frames G and H are enlargements of a region in frame F and show that fluorescence is present in the cytoplasm.

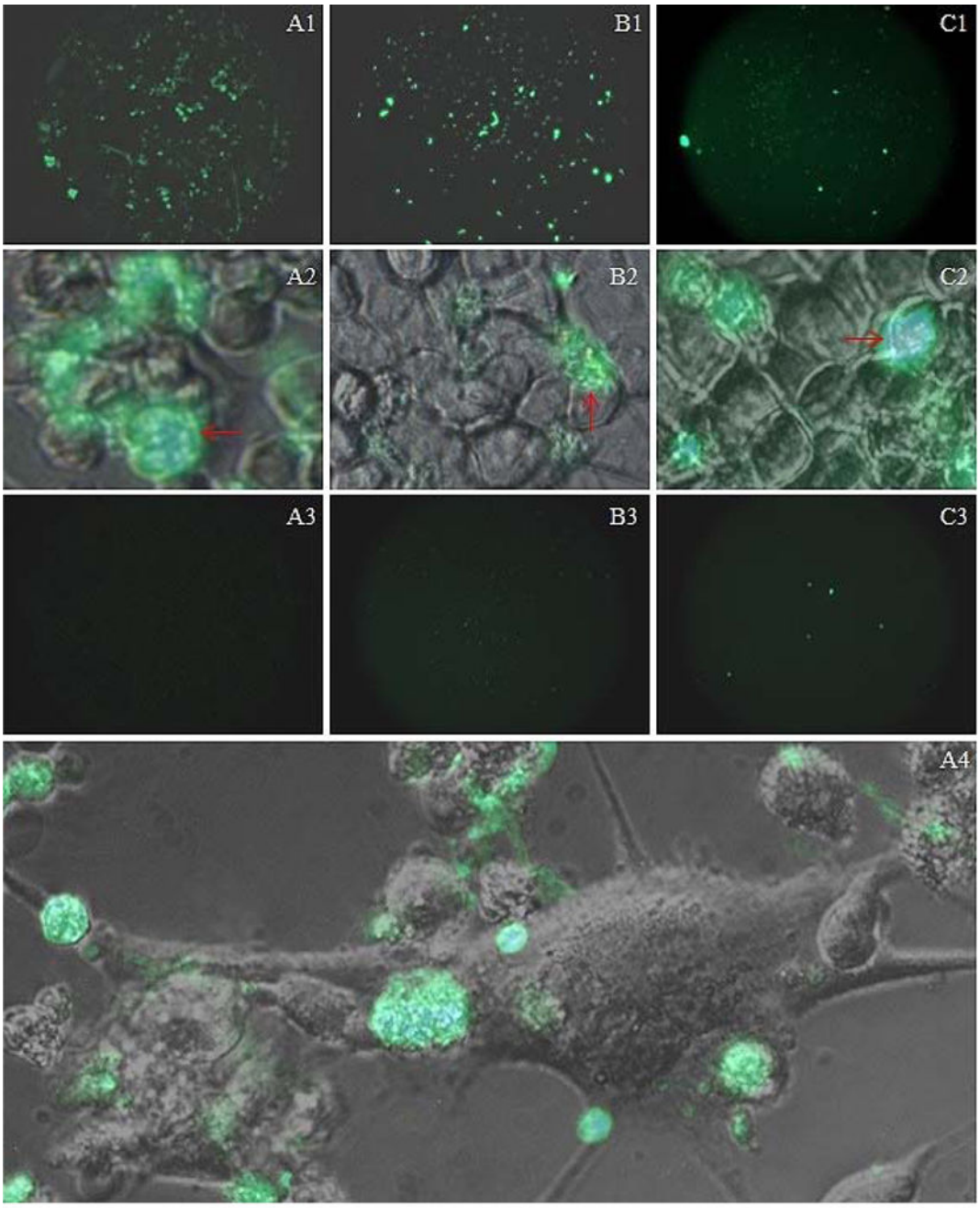

A.

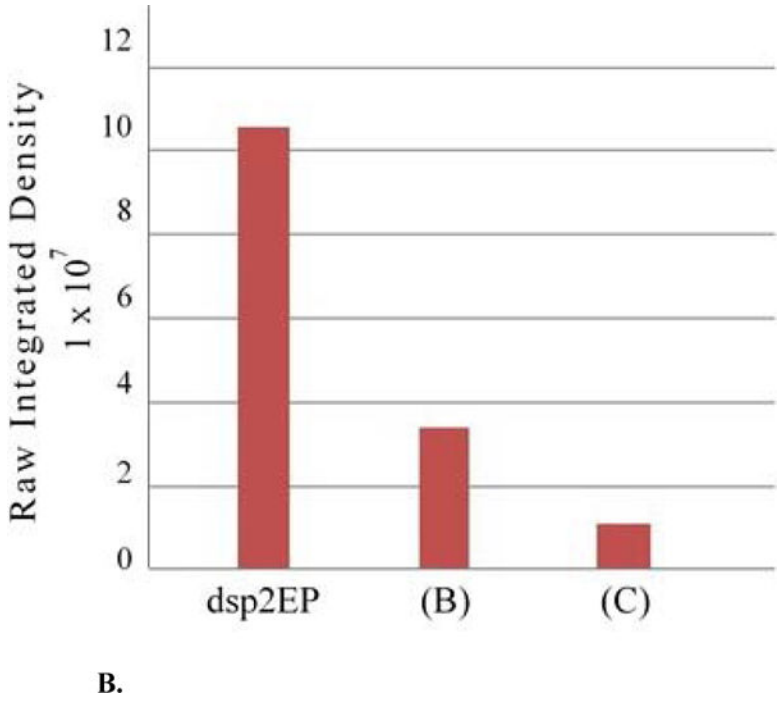

Figure 2. HeLa cell binding of Dsp2EP-FITC compared to mutated peptides Dsp2EP (B)-FITC and Dsp2EP(C)-FITC

Briefly, 1 mg of peptide was solubilized in 1 mL PBS and $MgCl_2$ in microfuge vials. Each was centrifuged to clarity and 30 μL of the solution was added to cells. A) Images in frames A1, B1, and C1 show green fluorescence of Dsp2EP, Dsp2EP (B), and Dsp2EP (C), respectively, bound to cells. Overlays A2, B2, and C2 are enlarged regions of A1, B1 and C1 with their corresponding bright field images. Red arrows indicate loci that suggest clustering of labeled peptide. Images A3, B3, and C3, repeat cultures of those in top row, show fluorescence quenched using Trypan Blue dye. Enlarged overlay in frame A4 shows that Dsp2EP-FITC appears in clusters on the cell surface. B) Comparison of raw integrated densities for images A1, B1, and C1. Results were normalized based on absorbance at 494 nm. Results illustrate the importance of both RXXK and KXXK motifs in cell binding.

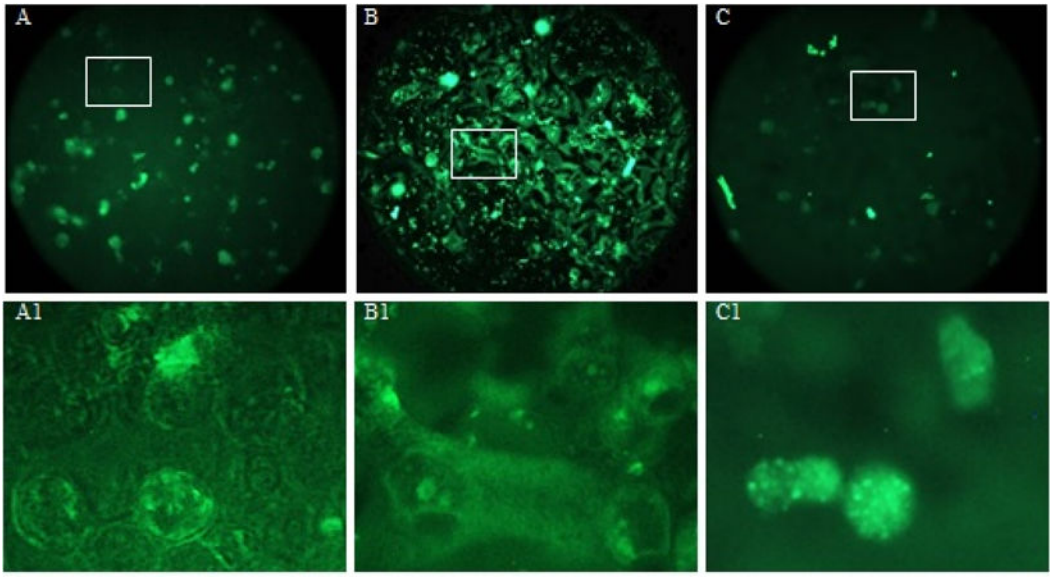

A.

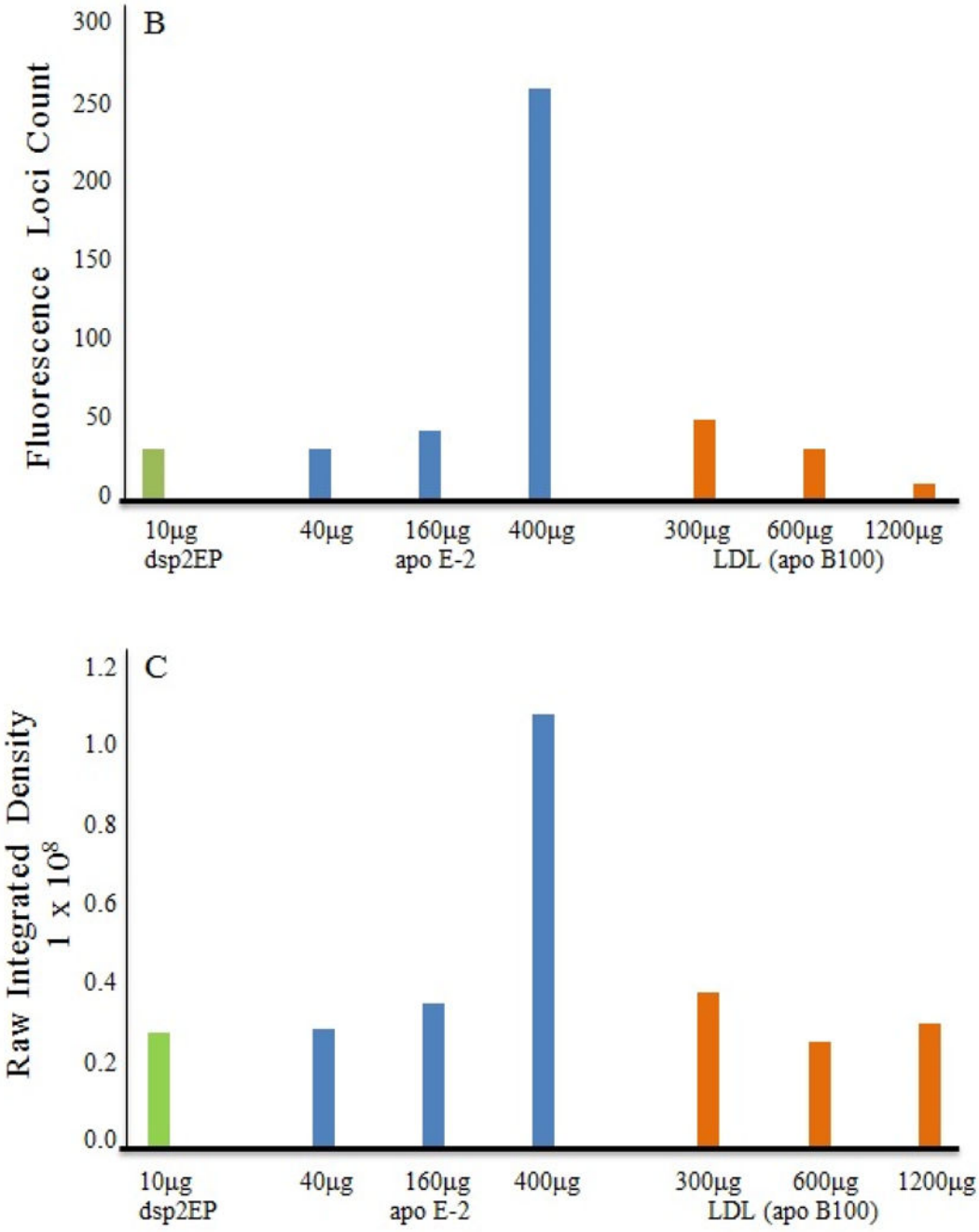

Figure 3. Effects of peptide E-2 and LDL on HeLa cell binding of Dsp2EP-FITC

A) Unlabeled E-2 (40 µg, 160 µg, 400 µg) was added to each culture containing 10 µg Dsp2EP in 500 µL PBS/ 5 mM MgCl2 and placed at 37° C for 18 hours. Parallel assays were performed using unlabeled human LDL (300 µg, 600 µg, 1200 µg) in lieu of E-2. Representative images obtained for experiments Dsp2EP-FITC alone, plus peptide E-2, and plus LDL are shown in frames A, B, and C, respectively. Enlarged images A1, B1, and C1 are of areas indicated in corresponding frames and show fluorescence signal in clusters on the cell surface. B) Number of points (loci) of signal for images in frames A, B, and C of

Fig. 3A. C) Total Raw Integrated Densities for the same frames A, B, and C in Fig. 3A. Image J software was used to count loci and integrate the fluorescence signal. The number of fluorescing loci and integrated density values for cells treated with 10 μg Dsp2EP-FITC alone are shown in green columns, Dsp2EP-FITC plus unlabeled E-2 peptide – in blue, and Dsp2EP-FITC plus unlabeled purified human LDL are in orange. Amounts of E-2 peptide or LDL used in the assays are shown under each column. E-2 peptide at high concentration significantly enhances binding of Dsp2EP-FITC to HeLa cells which appears to be ubiquitous, frame B in Figure 3A.

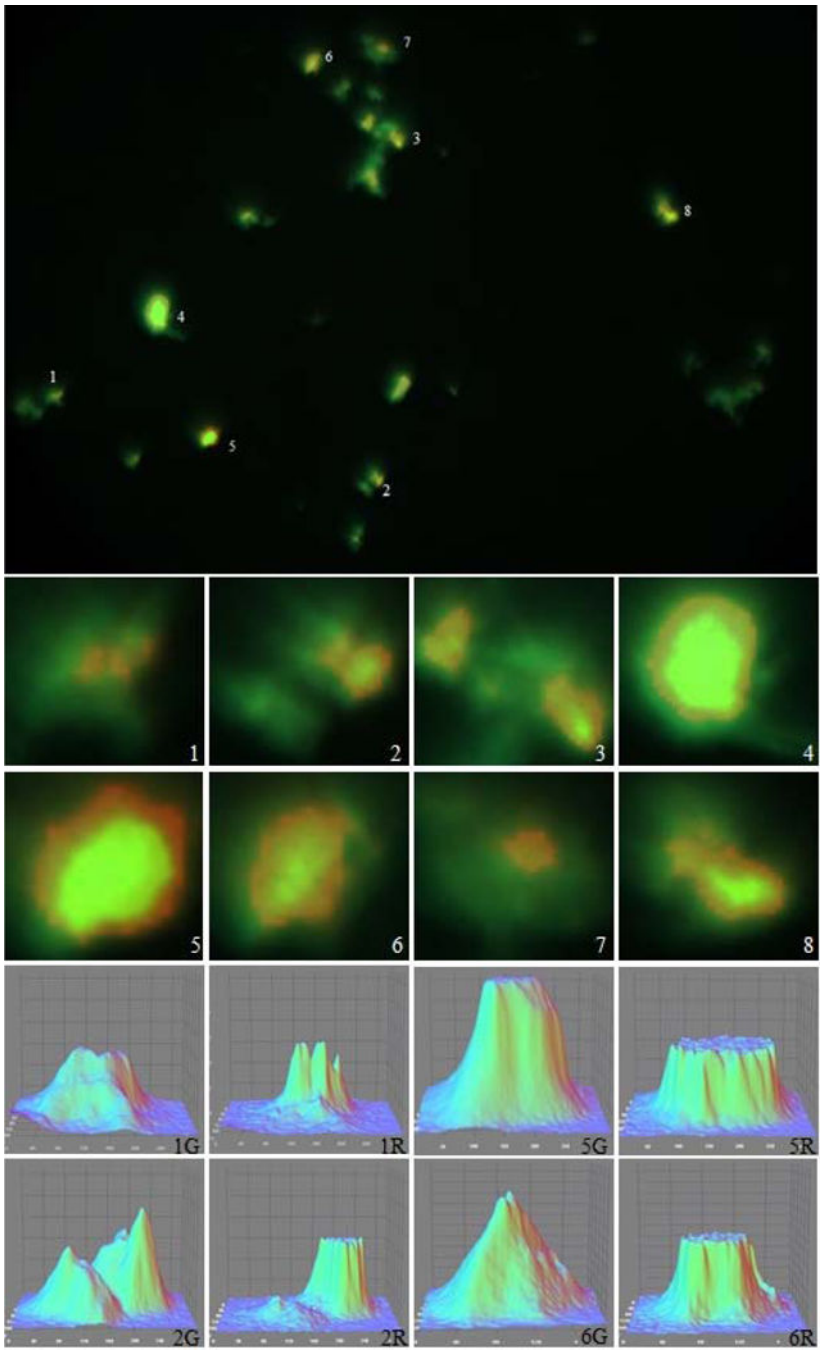

Figure 4. Dual label HeLa cell binding experiments using Dsp2EP-FITC and Apo E-CM-DiI

Overlay of Dsp2EP-FITC (green fluorescence) and Apo E-CM-DiI (red fluorescence), frame A, shows co-localized signals in yellow. Images of areas labeled 1 – 8 of the overlay image were enlarged in Photoshop then analyzed with ImageJ. Image 1 shows diffused signal for Dsp2EP-FITC (green) with clusters of red signal indicating Apo E-CM-DiI. Images in frames 1 – 8 reveal a consistent pattern, i.e. diffused (spread) binding of Dsp2EP-FITC and clustering of Apo E-CM-DiI. Red and green colors were separated using Image J and then rendered using Interactive 3-D Surface Plot Plugin algorithm. Images 1G and 1R represent

green and red signals, respectively. Images 1R, 2R, 5R and 6R represent Apo E-CM-DiI and show formation of clusters of similar intensity. Corresponding green signal images show less uniformity.

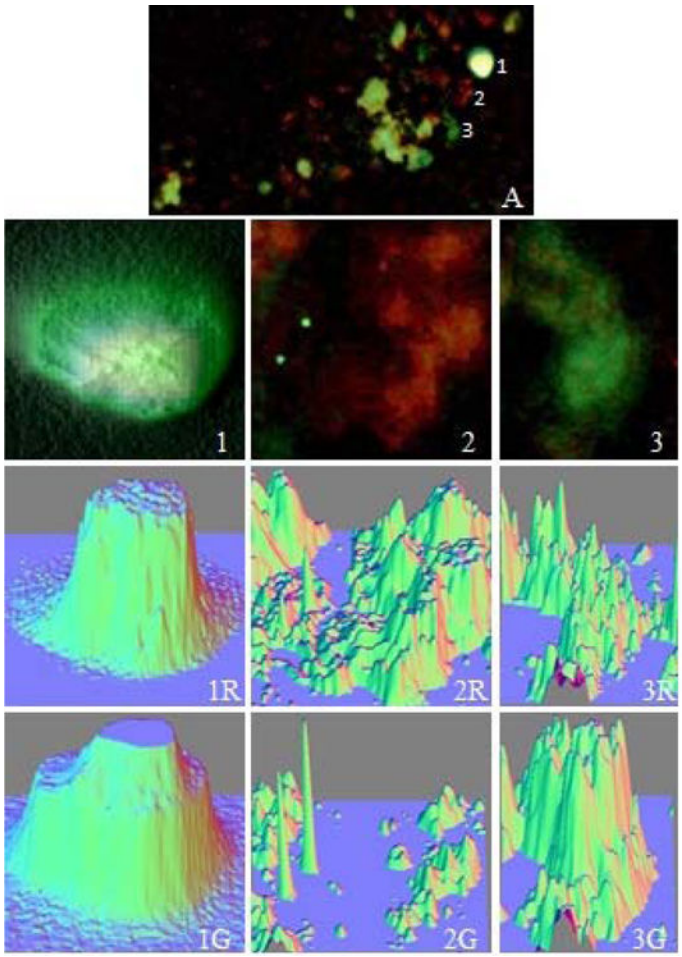

Figure 5. Dual label HeLa cell binding experiments using Dsp2EP-FITC and LDL-CM-DiI

Overlay A shows images of Dsp2EP-FITC (green) and LDL-CM-DiI (red) fluorescence images. Loci 1, 2, and 3 indicated in frame A are shown as enlarge images in frames 1, 2, and 3, respectively. Signals in locus frame 1 appear in three distinct colors, yellow, pink and green. Red is the predominant signal in locus A2, frame 2, while green signal is seen in locus A3, frame 3. ImageJ was used to separate green and red signals, rendered in 3D in corresponding frames 1R and 1G, 2R and 2G, and 3R and 3G, respectively.

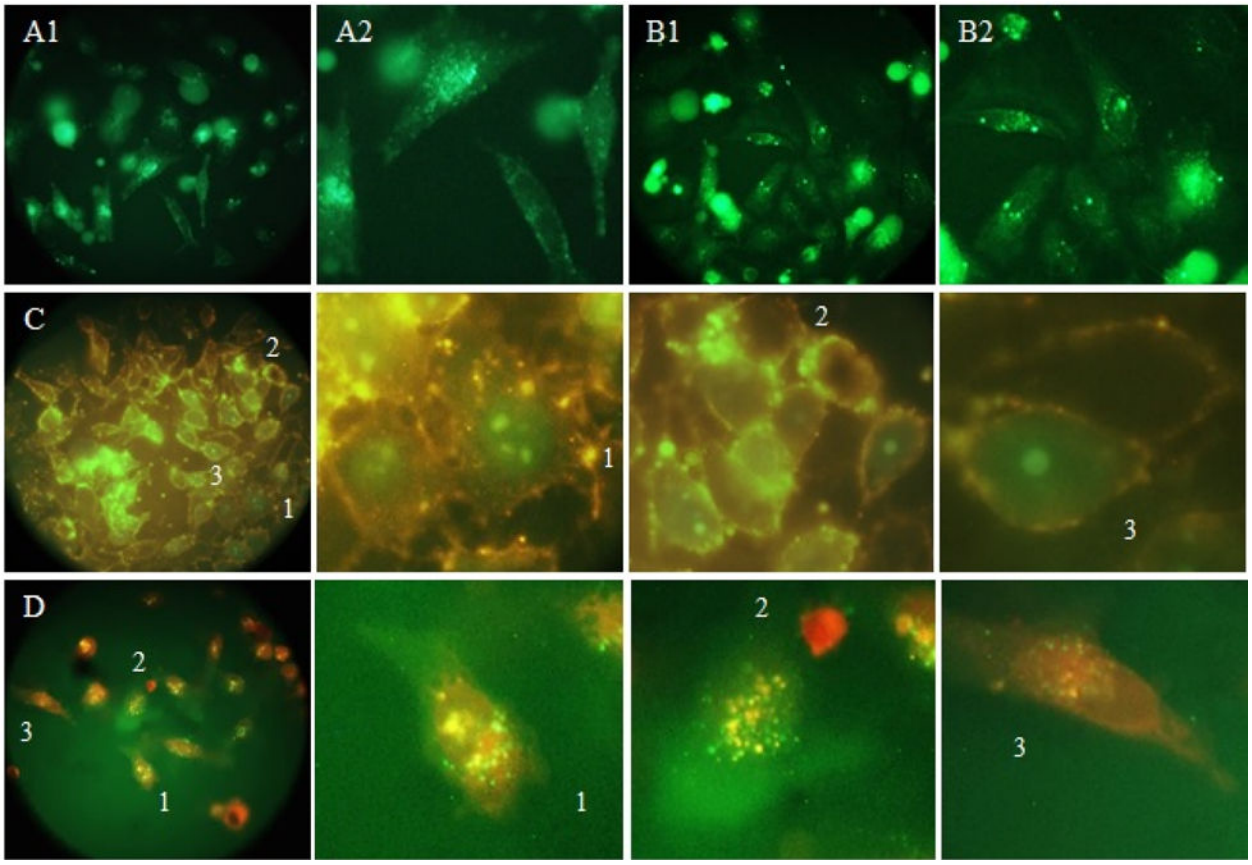

Figure 6. HeLa cell entry and nuclear translocation of Dsp3CP-FITC

Image in frame A1 shows cell uptake and nuclear translocation of Dsp3CP-FITC alone. Image A2 an enlarged region of A1 shows fluorescence suggestive of endosome-like structures and clusters in and about the nuclear space. Image B2 shows location of Dsp3CP-FITC signal in the presence of apo E-2 peptide. Image B2, an enlarged region of B1, also shows evidence that Dsp3CP-FITC signal occurs in endosomes and the nuclear space apparently unaffected by the addition of unlabeled Apo E-2 at 1.5 molar excess. Images in rows C and D were obtained in dual label experiments using 24 μL of Dsp3CP-FITC (50 μg) and apo E-CM-DiI (75 μg) mix. Apo E-CM-DiI-and Dsp3CP-FITC were added to live HeLa cells in FBS-depleted EMEM then incubated at ambient temperature for 15 and 90 minutes, C and D series, respectively. Areas 1, 2 and 3 in image C are enlarged to show typical colocalized signals on the cell membrane. Green signal is also clearly appears in the nucleus at this early time point. In D, signals appear separate as well as colocalized within the cell perimeter. Interestingly, FITC signal appears to be dispersed both within the cell and in the extracellular space while Apo E CM-DiI signal is indicated mostly within the cells. Cell nuclei appear to contain both green and red label.

Table 1

LDL Receptor Ligand and NLS Motifs in Apo E Sequence.

Type I	***Type II***	***Type III***	***Mono NLS***	***Bi-partite NLS***
XBBBXXBX	**XBBXBK**	**ΨBΨXBX**	**XBBBX**	**BBXXXXXXXXXXBXBXB**
LRKRLLRD	LR**K**LRK	L**K**AY**K**S	**RK**L**RKR**	**R**V**R**LASHL**RK**L**RKR**LL**R**
		A**R**LS**K**E	E**RL**A**R**	**RLRAR**MEEMGS**RT**D**R**
			S**RT**D**R**	
E131 peptide		^{0131}EEL**RVR**LASHL**RK**L**RKR**LL**R**DADDLQ**KR**LAVYQAGA**R**EGAE**R**G^{0173}-K-FITC		
Apo E-2 peptide		NH2-STEEL**RVR**LASHL**RK**L**RKR**LL**R**DADDLQ**KR**LAVYTQHG-OH		

Table 2

Receptor Ligand and NLS Motifs in the Dengue Virus Envelope Proteins.

Envelope Proteins	Potential Receptor Ligand and Nuclear Localization Signal Motifs		
	ΨBΨXB	mono	bipartite
DENV2	L**R**MD**K**	L**K**C**R**L**R**M	**KK**GSSIGQMFETTM**R**GA**KR**
	F**K**IV**K**	M**R**GA**KR**M	
Dsp2EP	^{0564}KCRL**R**MD**K**LQLKGMSYSMCTGKF**K**IV**K**EIAET-K-FITC		
Dsp2EP(B)	^{0558}GHLKCRLDMDDLQLKGMSYSMCTGKF**K**IV**K**EIAETQHG-K-FITC		
Dsp2EP(C)	^{0558}GHLKCRL**R**MD**K**LQLKGMSYSMCTGKFDIVDEIAETQHG-K-FITC		
	Receptor Ligand Motifs in Dsp2EP, Apo E and Apo B100		
DENV2EP	^{0563}L**K**C**R**L**R**MD**K**LQL**K**G-MSYSMCTG**K**F**K**IV**K**EIAET^{0595}		
Apo E	^{0067}TM**K**EL**K**AY**K**SELEEQLTPVAEET**R**A**R**LS**K**ELQAA0100		
Apo B100	^{3176}FD**R**HFE**K**N**R**NNALDFVT**K**SYNET**K**I**K**FD**K**Y**K**AE**K**3209		
Apo B100	^{3181}E**K**N**R**NNALDFVT**K**SYNET**K**I**K**FD**K**Y**K**AE**K**SHDEL3214		
Apo B100	^{2604}NF**K**DL**K**NI**K**IPS**R**FSTP(X_{18})EM**K**V**K**II**R**TIDQM^{2651}		

Table 3

Receptor Ligand and NLS Motifs in Amino-Terminus of Dengue Virus 3 Capsid Protein.

Capsid Proteins	Potential Receptor Ligand Motifs			Potential Nuclear Localization Signal	
	X**BBB**XX**B**X (I)	X**BB**X**B**X (II)	ψ**B**ψX**B** (III)	mono	bipartite
DENV3	Q**RKK**TG**K**P	L**KR**V**R**N	I**K**VL**K**G	**RKK**TG**K**	**RKK**TG**K**PSINML**KR**V**R**N
Capsid			L**K**GF**KK**	**KR**V**R**N**R**	**KK**EISNMLSIIN**KRRK**T
				KRFS**R**G	
				RGF**KK**E	
Dsp3CP	^{0002}NNQ**RKK**TG**K**PSINML**KR**V**R**N**R**VSTGSQ^{0028}-K-FITC				
ApoE	^{0142}**RK**L**RKR**LL**R**DADDLQ**KR**LAVYQAGA**R**E^{0168}				
ApoB100	^{3358}**R**LT**RKR**GL**K**LATALSLSN**K**FVEGSHNS^{3384}				

Table 4

Envelope Proteins	Potential Receptor Ligand Motifs	Potential Nuclear Localization Signal
	ΨBΨXB -loop- ΨBΨXB	*Bi-Partite*
DENV1	^{0563}L**K**C**R**L**K**MD**K**LTL**K**GVSYVMCTGSF**K**LE**K**EV^{0592}	^{0673}**KK**GSSIG**K**MFEATA**R**GA**RR**
DENV2	0563L**K**C**R**L**R**MD**K**LQL**K**GMSYSMCTG**K**F**K**IV**K**EI^{0592}	^{0673}**KK**GSSIGQMFETTM**R**GA**KR**
DENV3	^{0561}L**K**C**R**L**K**MD**K**LEL**K**GMSYAMCTNTFVL**KK**EV^{0590}	^{0671}**KK**GSSIG**K**MFEATA**R**GA**RR**
DENV4	^{0558}L**K**C**K**V**R**ME**K**L**R**I**K**GISYTMCSG**K**FSID**K**EM^{0587}	^{0668}**RK**GSSIG**K**MFESTY**R**GA**KR**

DENV1, BAD42414.1; DENV2, ACY70846.1; DENV3, ADI80662.1; DENV4, AAW51421.1